

Beating phenomena in spacecraft sine testing and an attempt to include the sine sweep rate effect in the test-prediction

Pietro Nali*¹ and Alain Bettacchioli²

¹Thales Alenia Space Italy, Strada antica di Collegno, 253 - 10146, Turin, Italy

²Thales Alenia Space France, 5 Allée des Gabians - 06150 Cannes, France

(Received September 1, 2015, Revised October 21, 2015, Accepted October 31, 2015)

Abstract. The Spacecraft (S/C) numerical sine test-predictions are usually performed through Finite Element Method (FEM) Frequency Response Analysis (FRA), that is the hypothesis of steady-state responses to harmonic excitation to the S/C base is made. In the test practice, the responses are transient and may be significantly different from those predicted through FRA. One of the most significant causes of discrepancy between prediction and test consists in the beating phenomena. After a brief overview of the topic, the typical causes of beating are described in the first part of the paper. Subsequently, focus is made on the sine sweep rate effect, which often leads to have beatings after the resonance of weakly damped modes. In this work, the approach illustrated in the literature for calculating the sine sweep rate effect in the case of Single-Degree-Of-Freedom (SDOF) oscillators is extended to Multi-Degrees-Of-Freedom (MDOF) systems, with the aim of increasing the accuracy of the numerical sine test-predictions. Assumptions and limitations of the proposed methodology are detailed along the paper. Several assessments with test results are discussed and commented.

Keywords: sine sweep rate effect; sine test-predictions; beating phenomena; sine testing; FRA

1. Introduction

Low-frequency base-shake sine tests, hereafter shortly called sine tests, are usually performed in the aerospace industry for identifying the modal characteristic, qualifying the structural design and verifying the structural integrity of S/Cs and related subsystems (Wijker 2004, Girard and Roy 2008, Lalanne 2009). It is understood that the numerical sine test-predictions play a significant role in the qualification process for low-frequency environment. Numerical sine test-predictions are usually made through the use of the FRA. This implies the hypothesis of system linearity and steady-state responses. In this work the hypothesis of system linearity is retained, while the appropriateness of the hypothesis of steady-state responses is discussed.

Sine tests are generally operated by providing swept excitations to the base of the structure under test. During the swept sine tests, there are many circumstances where the steady-state hypothesis is not verified or represents a strong approximation. For example, this happens when there is the occurrence of beating phenomena, which cannot be predicted by FRA and might lead

*Corresponding author, Ph.D, E-mail: pietro.nali@thalesaleniaspace.com

to unexpected oscillations or overshoots during the test (Naisse and Bettacchioli 2012). For this reason, the prediction of beating phenomena would represent an enhancement of the numerical sine test-prediction activity.

Sec. 2 provides an overview of the most common causes of beating in vibration testing.

The remaining part of the work is devoted to the prediction of the beating phenomenon described in Sec. 2.3, which typically occurs in case of swept sine tests of weakly damped structures. In these cases, the error due to the steady-state assumption mainly depends on the frequency of interest, the sine sweep rate employed and the damping of the structure under test. For the sake of clarity, the above numerical discrepancy will be indicated hereafter like “sine sweep rate effect”.

The majority of S/C system/subsystem qualification or acceptance sine tests are performed with a sine sweep rate between 2 and 4 [oct/min]. In the common practice, the sine sweep rate effect is noticeable with a sine sweep rate of 2 [oct/min] and it can become rather significant with 4 [oct/min] (ECSS-E-HB-32-26A 2013). As a consequence, the inclusion of the sine sweep rate effect in the numerical sine test-prediction is recommended by the authors when accurate evaluations are needed before the test campaign, e.g., in the case that a critical notching strategy has to be settled and agreed (a notching is a reduction of the input spectrum, see ECSS-E-HB-32-26A 2013 for additional details).

The effect that sine sweep rates have on the response amplitudes and on the estimation of resonant frequencies and damping has been quantified in the literature for SDOF oscillators (Lollock 2002, Roy and Girard 2012). The computational method proposed in the work by Lollock (2002) is recalled in Sec. 3. In Sec. 4 the same approach is extended to MDOF systems, providing a computational method to include the sine sweep rate effect in the numerical sine test-prediction. Reference to the mode superposition approach and basic structural dynamics is made (Craig 1981). Numerical results are obtained through a MATLAB[®] code implemented for the purpose. Two assessments with test results are discussed and commented in Sec. 5.

2. Typical causes of beating in vibration testing

During vibration tests, some oscillation problems typically appear around the main frequencies of resonance. Three different phenomena can explain these oscillations and they are described in the following Secs. 2.1-2.3.

2.1 Beating from two close-frequency oscillations

This phenomenon appears if the same structure is excited in the same point by the persisting superposition of two excitations having nearly the same frequency content (e.g., caused by two tuning forks). For example, if the two excitations are sinusoidal and of unitary amplitude, the resulting forcing excitation reaches the maximal value of two and can be expressed through the first prosthaphaeresis formula, leading to Eq. (1). That is, the structure undergoes vibrations of frequency equal to the half of the frequencies sum, which are modulated by a function having frequency equal to the half of the frequency difference, see Fig. 1.

$$\sin(2\pi f_1 t) + \sin(2\pi f_2 t) = 2 \cos[\pi(f_1 - f_2)t] \sin[\pi(f_1 + f_2)t], \quad (1)$$

where f_i is the i th frequency and t is the time.

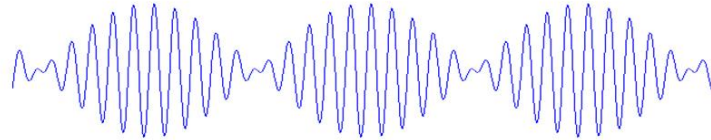


Fig. 1 Example of beating resulting from the superposition of two close-frequency sinusoidal excitations

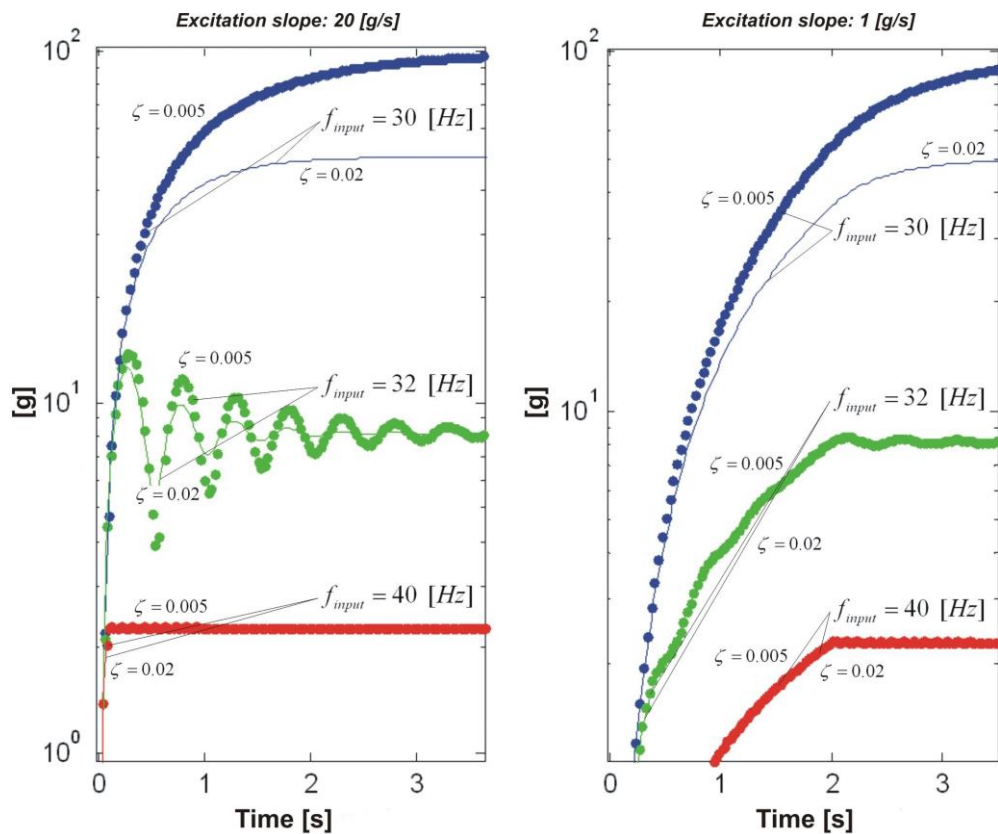


Fig. 2 SDOF oscillator response amplitudes with varying ζ , f_{input} and initial excitation slope; $f_n = 30$ [Hz]

This type of beating is quite rare in sine testing since the main resonant frequencies of the structures under test are typically not sufficiently close between each other.

2.2 Beating from transient excitation with frequency content close to a resonant frequency

Weakly damped structures undergoing an input composed by sine excitations with frequency close to a system resonance can experience the beating phenomenon if the excitation level is applied suddenly or is modulated with a fast rise time. As an example, a SDOF oscillator having natural frequency $f_n = 30$ [Hz] is considered in Fig. 2, which is composed by two subfigures.

Both subfigures provide results obtained imposing as input a sinusoidal excitation of specified frequency f_{input} and setting the initial conditions of null displacement and unitary velocity. The amplitude of the input excitation is of 1 [g], being g the standard value of gravitational acceleration. Exception is made for the initial rise of excitation, where the input passes from 0 [g] to 1 [g], with a constant excitation slope of 20 [g/s] and 1 [g/s], respectively in the left and right subfigure. Red, green and blue curves are obtained by setting f_{input} to 40 [Hz], 32 [Hz], and 30 [Hz], in the same order. Both damping ratios ζ of 0.02 and 0.005 are considered. Each curve shows how the response amplitude evolves with the time. It is confirmed that, once the steady-state condition is reached, the response amplitude is constant, while the beating phenomenon can appear only around the initial transient phase. It can be noted that the beating is more accentuated in the case of high excitation slope, small damping ratio and when the f_{input} is slightly higher than f_n . This is the typical condition occurring in S/C sine testing in case of positive sweep, when the swept sine excitation passes the first main mode and the excitation level rises after the notching. It is the case recalled by Fig. 10, where the corresponding excitation slope is about 0.25 [g/s] and the natural frequency of interest is around 16 [Hz]. The transient phenomenon described in this section is partially responsible of the overshoot visible in the test result curve of Fig. 10. The more visible oscillations are mainly due to a different cause of beating which is described in Sec. 2.3.

2.3 Beating due to sine sweep rate

The sine sweep rate might be the most relevant cause of beating during the standard sine tests. A complete overview and description of the sine sweep rate effect for SDOF oscillators is provided by works Lollock (2002), Nali and Calvi (2006), Calvi and Nali (2007), Roy and Girard (2012). The sine sweep rate effect can be identified in Figs. 3-6, which illustrate several swept responses of SDOF oscillators for both up and down directions of frequency sweep. The ratio \ddot{U}/\ddot{Z} is on the ordinate axis, where \ddot{U} indicates the acceleration response amplitude and \ddot{Z} indicates the amplitude of the imposed swept acceleration to the base. Sec. 3.2 describes how the curves in Figs.

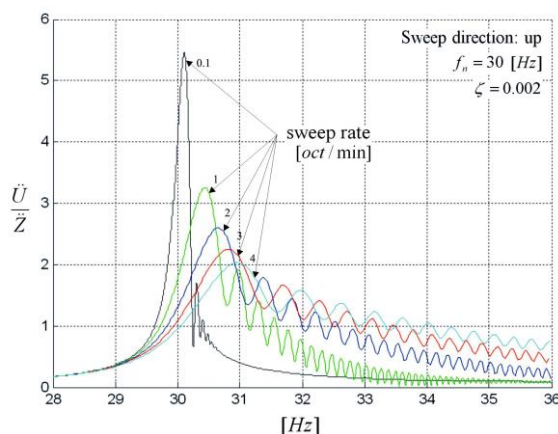


Fig. 3 SDOF oscillator transient swept acceleration responses with various sine sweep rates, sweep up, $f_n = 30$ [Hz], $\zeta = 0.002$

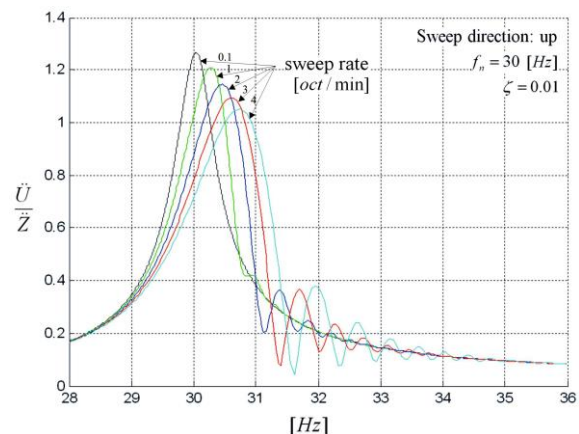


Fig. 4 SDOF oscillator transient swept acceleration responses with various sine sweep rates, sweep up, $f_n = 30$ [Hz], $\zeta = 0.01$

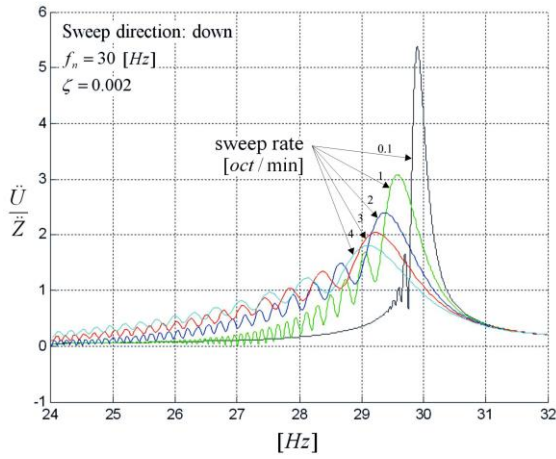


Fig. 5 SDOF oscillator transient swept acceleration responses with various sine sweep rates, sweep down, $f_n = 30$ [Hz], $\zeta = 0.002$

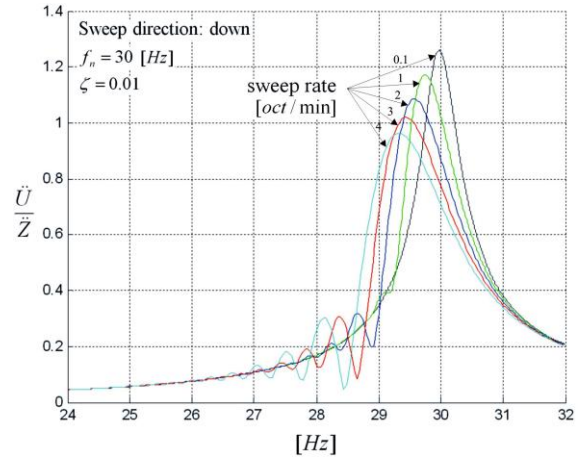


Fig. 6 SDOF oscillator transient swept acceleration responses with various sine sweep rates, sweep down, $f_n = 30$ [Hz], $\zeta = 0.01$

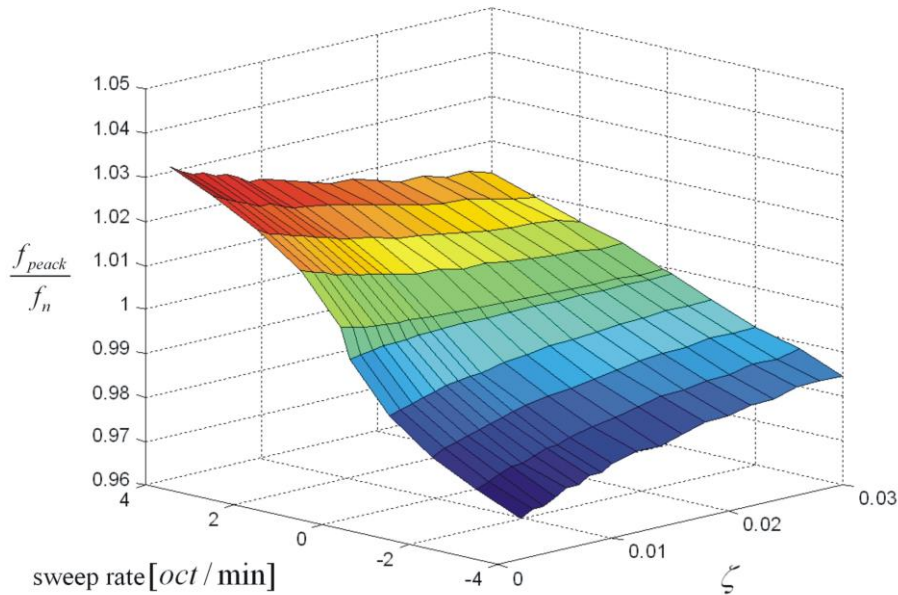


Fig. 7 Normalized frequency of the first peak of beating as a function of the sine sweep rate and ζ

3-6 are calculated. Sweeps of exponential type (see Eq. (8)) are considered. It should be noted that, in this case, the beatings always appear just after crossing the resonant frequency. Moreover, the amplitude and the duration of the beatings become more significant with higher sine sweep rates and lower damping ratios. Fig. 7 shows the frequency of the first peak of beating, normalized with respect to f_n , as a function of the sine sweep rate and of ζ . The figure shows that, if the sweep rate is positive, by increasing it, the frequency of the first peak of beating increases as well. Moreover, if the sweep rate is negative, by decreasing it, the frequency of the first peak of beating

decreases. In case of positive sweep rates, when ζ decreases, the first peak of beating increases. Differently, in case of negative sweep rates, when the ζ decreases, the first peak of beating decreases as well.

2.4 Beating or instabilities?

Without going into the details of the common algorithms used for the vibrators control, it should be underlined that, during sine tests, the closed-loop control may lead to instabilities which are typically sensitive to a parameter called compression factor. The control algorithm considers the compression factor in order to evaluate the rate at which the errors in the control signal can be corrected by the system. Low values of compression factors allow “immediate” corrections, while high values of it provide more “soft” adjustments, leading to a control process slower but more stable. In other words, if the compression factor is high enough, the subsequent low-pass filter effect tends to stabilize the system. In this case, the beatings which can be observed are similar to those that would be obtained with open-loop excitations. Conversely, with a low compression factor, the control system becomes faster and more reactive. This is apparently an advantage, but it has the drawback that a fast dynamics easily leads to instabilities. A good test practice is to adjust the compression factor through a trade-off, with the objective of obtaining a control reactive enough to minimize the errors and retaining, at the same time, the stability of the system. Such trade-off might be performed by executing a few low level runs, each one with a different choice of compression factor, and comparing the test responses.

It should be remarked that possible test-aborts are primarily due to sensors’ overshoots overpassing the corresponding threshold of abort and this mainly happens in case of instabilities.

3. Base motion of SDOF oscillator

The complex equation for the absolute motion of the SDOF oscillator, with moving base and when no external force is applied to the mass, is given below (Craig 1981, Nali *et al.* 2013).

$$m\ddot{\bar{u}} + c\dot{\bar{u}} + k\bar{u} = c\dot{\bar{z}} + k\bar{z}, \quad (2)$$

where the overline indicates a complex quantity, \bar{u} is the displacement of the mass, \bar{z} is the displacement of the moving base and the dot denotes differentiation with respect to time. m , c and k are the mass, the coefficient of viscous damping and the spring constant, respectively. The hypothesis of linear oscillations is made.

3.1 Simple harmonic excitation to the base

If the base undergoes the simple harmonic motion $z = Z \cos(\Omega t)$, where Ω and t indicate respectively the excitation frequency and the time, moving to the complex domain implies that $z = \text{Re}(\bar{z}) = \text{Re}(Ze^{i\Omega t})$ where $i = \sqrt{-1}$ is the imaginary unit. The complex steady-state response $\bar{u} = \bar{U}e^{i\Omega t}$ is assumed.

It is convenient to divide Eq. (2) by m and rewrite it as

$$\ddot{\bar{u}} + 2\zeta\omega_n\dot{\bar{u}} + \omega_n^2\bar{u} = 2\zeta\omega_n\dot{\bar{z}} + \omega_n^2\bar{z}, \quad (3)$$

where ω_n is the undamped circular natural frequency and $\zeta = \frac{c}{c_{cr}}$ is the viscous damping factor, with $c_{cr} = 2\sqrt{km}$. \bar{U}/Z takes the following form

$$\frac{\bar{U}}{Z} = Tr\left(\frac{\Omega}{\omega_n}\right), \quad (4)$$

where

$$Tr\left(\frac{\Omega}{\omega_n}\right) = \frac{1 + 2i\zeta\frac{\Omega}{\omega_n}}{1 - \left(\frac{\Omega}{\omega_n}\right)^2 + 2i\zeta\frac{\Omega}{\omega_n}}. \quad (5)$$

The function $Tr\left(\frac{\Omega}{\omega_n}\right)$ in Eqs. (4) and (5) is commonly called transmissibility (Craig 1981). Since simple harmonic motion is considered, $\ddot{\bar{U}}/\ddot{Z}$ is given by the transmissibility function too.

3.2 Swept harmonic excitation to the base

For more details on the theoretical approach proposed in this section see the work by Lollock (2002).

The equation of relative motion of the SDOF oscillator can be written as it follows

$$\ddot{x} + 2\zeta\omega_n\dot{x} + \omega_n^2x = -\ddot{z}, \quad (6)$$

where $x = u - z$ is the relative displacement.

If swept excitations are provided to the base, it is convenient to express in the time-domain the corresponding swept base acceleration, according to the following form

$$\ddot{z} = \dot{Z}(t)e^{i\phi(t)}, \quad (7)$$

where $\dot{Z}(t)$ and $\phi(t) = \int_0^t \Omega(t) dt$ give respectively the amplitude and the phase angle of the base acceleration (Lollock 2012). $\Omega(t)$ indicates the instantaneous excitation frequency.

If an exponential sweep is considered

$$\Omega(t) = \Omega_0 2^{(K_e/60)t}, \quad (8)$$

where Ω_0 indicates the starting frequency of the sweep and the exponential sweep coefficient K_e is expressed in [oct/min].

If a linear sweep is imposed

$$\Omega(t) = \Omega_0 + (K_l/60)t, \quad (9)$$

where the linear sweep coefficient K_l is expressed in [rad/min].

Sweep up or down are obtained respectively with positive or negative values of K_e and K_l .

The following form for the SDOF response can be assumed

$$\bar{x} = \bar{X}(t)e^{i\phi(t)}. \quad (10)$$

By substituting Eqs. (7) and (10) into Eq. (6), and keeping implicit the indication of time-

functions for sake of notation, leads to

$$\ddot{\bar{X}} + (2i\dot{\phi} + 2\zeta\omega_n)\dot{\bar{X}} + (i\ddot{\phi} - \dot{\phi}^2 + 2\zeta\omega_n i\dot{\phi} + \omega_n^2)\bar{X} = -\ddot{Z}. \quad (11)$$

By substituting $\bar{X} = R + iV$, Eq. (11) can be rewritten in terms of real and imaginary components

$$\ddot{R} + \dot{R}(2\zeta\omega_n) + R(\omega_n^2 - \dot{\phi}^2) - \dot{V}(2\dot{\phi}) - V(\ddot{\phi} + 2\zeta\omega_n\dot{\phi}) = -\ddot{Z}, \quad (12)$$

$$\dot{V} + \dot{V}(2\zeta\omega_n) + V(\omega_n^2 - \dot{\phi}^2) + \dot{R}(2\dot{\phi}) + R(\ddot{\phi} + 2\zeta\omega_n\dot{\phi}) = 0. \quad (13)$$

The fourth-order ordinary differential system given by Eqs. (12) and (13) can be solved through classical numerical methods. The following initial conditions limit the starting oscillations in the solution

$$\begin{aligned} R &= \text{Re} \left[\text{Tr} \left(\frac{\Omega_0}{\omega_n} \right) \right] \cdot \left(-\frac{\ddot{Z}}{\omega_n^2} \right); \\ V &= \text{Im} \left[\text{Tr} \left(\frac{\Omega_0}{\omega_n} \right) \right] \cdot \left(-\frac{\ddot{Z}}{\omega_n^2} \right); \\ \dot{R} &= 0; \dot{V} = 0. \end{aligned} \quad (14)$$

After solving the system by Eqs. (12) and (13), $\left| \ddot{U}/\ddot{Z} \right|$ can be calculated as it follows

$$\left| \frac{\ddot{U}}{\ddot{Z}} \right| = \frac{|\ddot{x} + \ddot{z}|}{|\ddot{z}|}, \quad (15)$$

where \ddot{x} is given by the second derivative of Eq. (10) with respect to time:

$$\ddot{x} = \left[(\ddot{R} - 2\dot{\phi}\dot{V} - \ddot{\phi}V - \dot{\phi}^2R) + i(\dot{V} + 2\dot{\phi}\dot{R} + \ddot{\phi}R - \dot{\phi}^2V) \right] e^{i\phi(t)}. \quad (16)$$

$\left| \ddot{U}/\ddot{Z} \right|$ provides the amplitude ratio between the acceleration of the mass and the acceleration imposed to the base, in the time-domain. The sine sweep rate effect can be thus quantified by comparing $\left| \ddot{U}/\ddot{Z} \right|$ from Eq. (15) with the transmissibility function of Eq. (4), being the passage from time-domain to frequency-domain given by Eq. (8) or (9), respectively in the case of exponential or linear sweep.

4. An attempt to calculate the sine sweep rate effect dealing with MDOF systems

If MDOF systems are addressed to, according to the mode superposition approach and structural dynamics basic theory (Sedaghati et al. 2003, Wijker 2004), in case of simple harmonic base motion excitation, the acceleration vector $\ddot{\mathbf{u}}$ is given by Eq. (17).

$$\ddot{\mathbf{u}} = \mathbf{\Phi} \ddot{\mathbf{z}} + \sum_{j=1}^n \mathbf{\Psi}_j \frac{1}{m_{jj} - 1 + \left(\frac{\omega_{nj}}{\Omega} \right)^2 + 2i\zeta_j \frac{\omega_{nj}}{\Omega}} \mathbf{L}_j \ddot{\mathbf{z}}, \quad (17)$$

where bold letters denote arrays and the subscript j indicates the relation with j th mode. $\ddot{\mathbf{z}}$ is the base motion excitation acceleration vector, Φ is the rigid-body matrix, Ψ_j is the j th fixed-base eigenvector, m_{jj} is the j th generalized mass and L_j is the j th mass modal participation factor.

By assuming that the eigenvectors are mass normalized leads to $m_{jj} = 1$. Moreover, by restricting the analysis only to the translational DOFs of $\ddot{\mathbf{u}}$, hereafter denoted with the subscript tr , and recalling the transmissibility ratio of Eq. (4) for the j th modal contribution, Eq. (17) becomes (Nali *et al.* 2013)

$$\ddot{\mathbf{u}}_{tr} = \left(\Phi_{tr} + \sum_{j=1}^n \Psi_j \left(Tr \left(\frac{\Omega}{\omega_{nj}} \right) - 1 \right) L_j \right) \ddot{\mathbf{z}}_{tr}. \quad (18)$$

The columns of Φ_{tr} are given by the translational rigid-body modes. A rigid-body mode corresponds to the displacement vector produced by imposing the unit value to a DOF of the moving base and setting the remaining DOFs of the moving base to zero. It follows that the cells of Φ_{tr} are null or of unitary absolute value, depending on the direction. In the latter case, the sign of the cell is given by the sign of the result of the summation in Eq. (18). By starting from Eq. (18) and substituting the function $Tr \left(\frac{\Omega}{\omega_{nj}} \right)$ with the ratio $\frac{\ddot{U}}{\ddot{Z}} \left(\frac{\Omega}{\omega_{nj}} \right)$, calculated for the j th mode and according to the approach in Sec. 3.2, the vector $\ddot{\mathbf{u}}_{tr}$ in the case of swept harmonic excitation can be calculated:

$$\ddot{\mathbf{u}}_{tr} = \left(\Phi_{tr} + \sum_{j=1}^n \Psi_j \left(\frac{\ddot{U}}{\ddot{Z}} \left(\frac{\Omega}{\omega_{nj}} \right) - 1 \right) L_j \right) \ddot{\mathbf{z}}_{tr}. \quad (19)$$

Fig. 8 shows the ratio $\left| \frac{\ddot{U}}{\ddot{Z}} \right|$ as a function of f and $f_j = 2\pi\omega_j$ in case of $\zeta = 0.01$ and exponential sweep up with rate of 3 [oct/min]. The figure illustrates the beating phenomenon due to the sine sweep rate effect described in Sec. 2.3.

5. Assessments with test results

The methodology proposed in Sec. 4 was implemented in the MATLAB[®] numerical computing environment¹. No dedicated sine tests were performed in the framework of the present work. However, some Thales Alenia Space pre-existing test results were addressed to in order to make some comparisons between numerical predictions and test results.

The first assessment is presented through Fig. 9 and pertains to a particular accelerometer present in the in-plane qualification sine test of a S/C subsystem. The test was performed with an exponential sweep up having the rate of 4 [oct/min]. The three following acceleration-curves are plotted.

- The FEM prediction without including the sine sweep rate effect, from Eq. (18), that is the result of the FEM FRA;

¹The MATLAB[®] code has to receive in input a MSC Nastran[™] .f06 file of the hard-mounted normal mode analysis of the structure to be tested.

- The FEM prediction with the inclusion of the sine sweep rate effect, from Eq. (19);
- The test result.

From the curves it is clear that the FEM model is not well correlated. This is particularly evident by looking at the main mode, in the range between 25 and 30 [Hz]. Apart the frequency shifts mainly due to correlation problems, for the purpose of this work, it can be noted that the beatings observed in the test after the main peak, just before 33 [Hz], are evident in the curve of the FEM prediction including the sine sweep rate effect, processed according to Eq. (19).

As illustrated in the work by Lollock (2002), the peak-frequency and the peak-amplitude of the swept-responses are sensitive both to the damping and to the sine sweep rate. As a consequence, it should be underlined that the correlation of the FEM model with the test data may be questionable if the sweep effect is not included in the FEM prediction and the test is performed with a high sine sweep rate.

The second assessment is presented through Fig. 10, which gives the input profile of a S/C qualification lateral sine test, performed with an exponential sweep up having the rate of 3 [oct/min]. Within the frequency range considered, the input profile was of 1 [g]. The decrease of the excitation level was due to the primary notching (see ECSS-E-HB-32-26A 2013 for additional info on primary notching). It can be stated that the proposed computational methodology which includes the sine sweep rate effect for MDOF systems is able to predict the beating oscillations occurring after 17 [Hz], with some minor dissimilarities mainly due to the fact that the test was conducted with a closed-loop control, in accordance with Sec. 2.4. In this case the compression factor was equal to 5, which is high enough to induce a low-pass filter effect, tending to stabilize the system and thus to attenuate the oscillations.

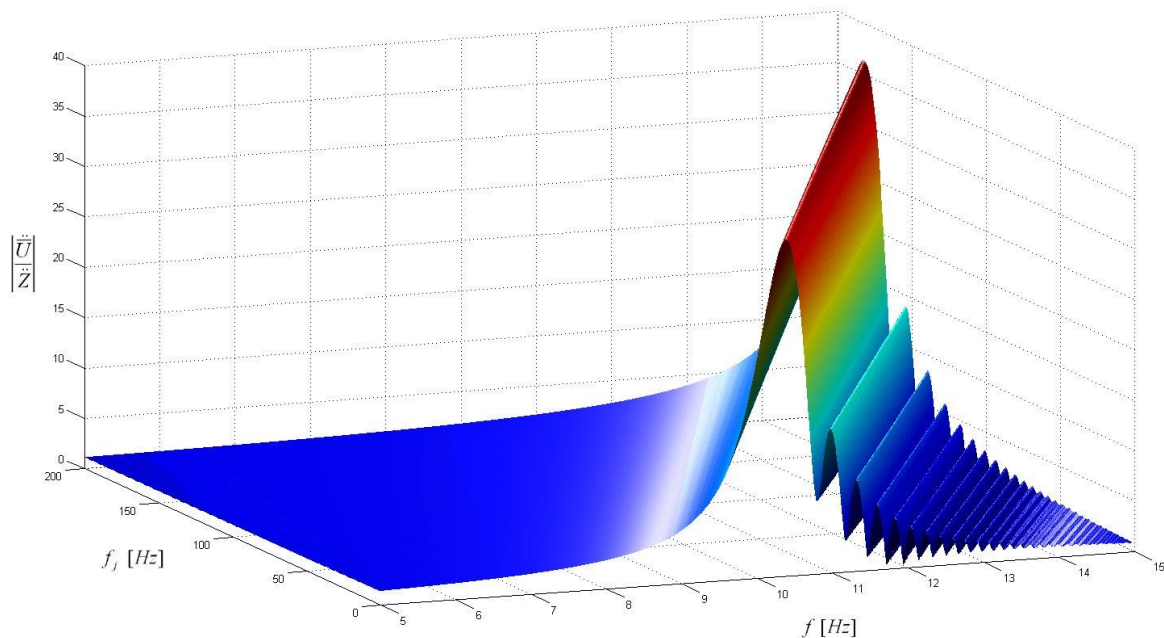


Fig. 8 $\left| \frac{\ddot{U}}{\ddot{Z}} \right|$ as a function of f and f_j with $\zeta = 0.01$ and exponential sweep up with rate of 3 [oct/min]. Related beatings are clearly visible after the resonance

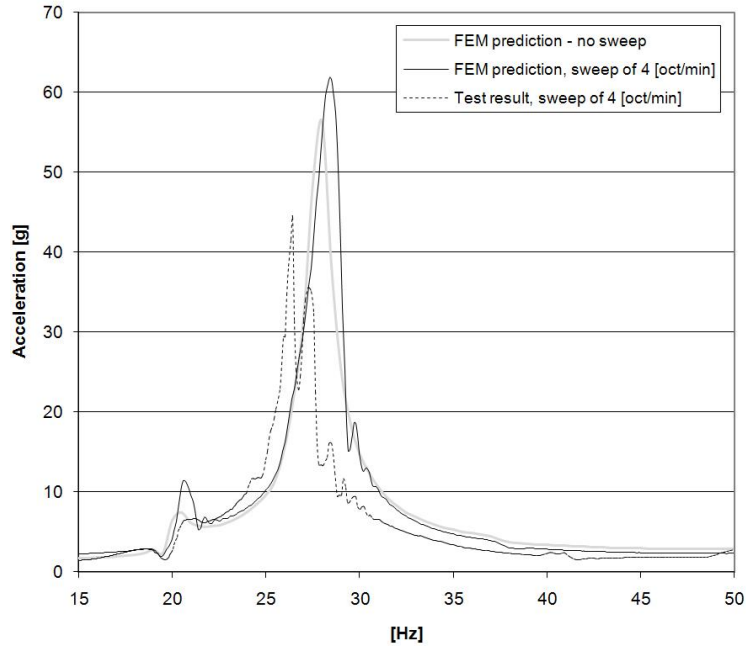


Fig. 9 Test results and FEM prediction, with and without the inclusion of the sine sweep rate effect

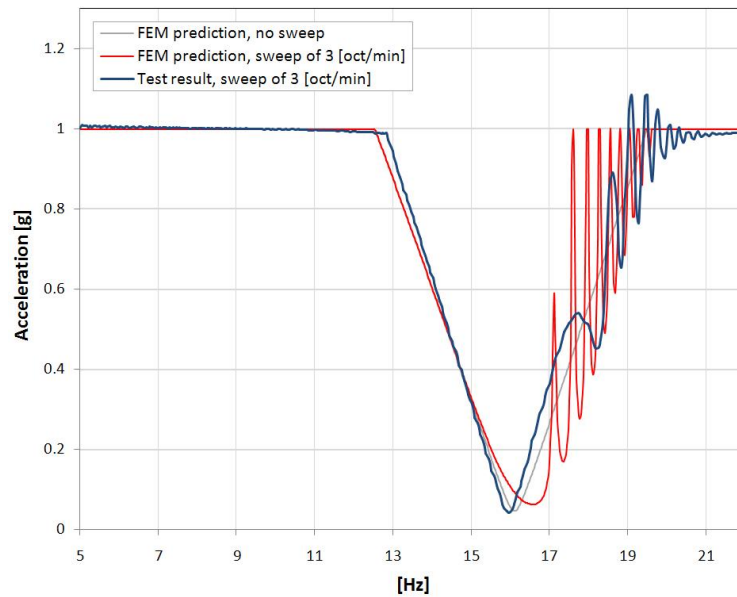


Fig. 10 Primary notched input profile of qualification lateral run. Test results and FEM prediction, with and without the inclusion of the sine sweep rate effect

Additional efforts on this topic are envisaged by the authors. Further comparisons between numerical predictions and *ad hoc* sine tests results, encompassing a variety of sine sweep rates would be recommended.

6. Conclusions

A brief overview of the most significant causes of beating in sine testing was presented in this work (Sec. 2). Several remarks based on common test practice and numerical simulations were reported in order to give an estimation of the probability to encounter, during sine tests, each one of the beating phenomena described. Particular attention was devoted to the beatings caused by the sine sweep rate, which represents a significant cause of discrepancy between the FEM prediction performed through FRA and the test results (Sec. 2.3). A numerical approach for calculating the sine sweep rate effect for SDOF systems was thus recalled from the literature (Sec. 3.2). Subsequently, a computational method aiming to extend the latter approach to MDOF systems by processing the results of the normal mode analysis was proposed (Sec. 4). Related assumptions and limitations were discussed. Comparisons between numerical predictions and available test results were made in order to assess the methodology presented (Sec. 5). In conclusion, the use of the computational method proposed in this work is recommended when the following conditions are verified: accurate numerical sine test-predictions are required; a weakly damped structure having relevant modes at low frequencies has to be tested; the sine tests have to be operated with relatively high sweep rates (sweep rates typically applied in S/C sine testing are between 2 and 4 [oct/min]; sweep rates of 3 and 4 [oct/min] are here considered high). Predicting the beatings due to the sine sweep rate before the test would facilitate the proper interpretation of the beating-peaks after the first test run.

An additional benefit of using of the here proposed methodology when testing S/Cs is to include the natural frequency shifts and the response amplitude variations due to the sine sweep rate in the sine test-prediction. This point can be relevant after the test, when discussing about the correlation of the FEM S/C model (and thus in the subsequent negotiation with the launch authority).

References

- Calvi, A. and Nali, P. (2007), "Some remarks on the reduction of overtesting during base-drive sine vibration tests of spacecraft", *ECCOMAS Conf. on Computational Methods in Structural Dynamics and Earthquake Engineering*, Rethymno, Crete, Greece, June.
- Craig, R.R. (1981), *Structural Dynamics, an Introduction to Computer Methods*, John Wiley & Sons.
- ECSS-E-HB-32-26A (2013), *Spacecraft Mechanical Loads Analysis Handbook*, ECSS Secretariat ESA-ESTEC Requirement & Standard Division, Noordwijk, The Netherlands.
- Girard, A. and Roy, N. (2008), *Structural Dynamics in Industry*, ISTE Ltd and John Wiley & Sons.
- Lalanne, C. (2009), *Mechanical Vibration & Shock Analysis, Vol 1: Sinusoidal Vibrations*, 2nd Edition, John Wiley & Sons.
- Lollock, J.A. (2002), "The effect of a swept sinusoidal excitation on the response of a single-degree-of-freedom oscillator", *43rd AIAA Structures, Structural Dynamics, and Materials Conference*, Denver, Colorado, March.
- Naisse, C. and Bettacchioli, A. (2012), "Simulation des essais en vibrations de satellites à partir de l'analyse modale d'une réponse bas niveau", A.S.T.E. n° 111.
- Nali, P. and Calvi, A. (2006), "An investigation on the spacecraft design loads cycles and sine vibration test", *TEC-MCS/2006/1362/In/AC*, ESA, Noordwijk, The Netherlands, March.
- Nali, P., Mucciante, L.D. and Caccamo, L. (2013), "An easy-to-implement computational method for the spacecraft sine test-prediction with particular emphasis on the modal contributions", *COMPADYN 2013*, Kos Island, Greece, June.

- Roy, N. and Girard, A. (2012), "Revisiting the effect of sine sweep rate on modal identification", *European Conference on Spacecraft Structures, Materials and Environmental Testing*, Noordwijk, The Netherlands, 20-23 March.
- Sedaghati, R., Soucy, Y. and Etienne, N. (2003), "Efficient estimation of effective mass for complex structures under base excitations", *Can. Aeronaut. Space J.*, **49**(3), 135-143.
- Wijker, J. (2004), *Mechanical Vibrations in Spacecraft Design*, Springer.

EC